European Journal of Medicinal Chemistry 58 (2012) 493–503

Contents lists available at SciVerse ScienceDirect

European Journal of Medicinal Chemistry

journal homepage: http://www.elsevier.com/locate/ejmech

Original article

Design, structural and spectroscopic elucidation, and the *in vitro* biological activities of new diorganotin dithiocarbamates

Isabella P. Ferreira [a], Geraldo M. de Lima [a,*], Eucler B. Paniago [a], Willian R. Rocha [a], Jacqueline A. Takahashi [a], Carlos B. Pinheiro [b], José D. Ardisson [c]

[a] Departamento de Química, Universidade Federal de Minas Gerais, UFMG, Avenida Antônio Carlos 6627, Belo Horizonte, MG, CEP 31270-901, Brazil
[b] Departamento de Física, Universidade Federal de Minas Gerais, UFMG, Avenida Antônio Carlos 6627, Belo Horizonte, MG, CEP 31270-901, Brazil
[c] Centro de Desenvolvimento em Tecnologia Nuclear, CDTN/CNEN, Avenida Antônio Carlos 6627, Belo Horizonte, MG, CEP 31270-901, Brazil

ARTICLE INFO

Article history:
Received 28 June 2012
Received in revised form
27 September 2012
Accepted 15 October 2012
Available online 24 October 2012

Keywords:
Biological activity
Organotin dithiocarbamate
Structural determination

ABSTRACT

The reaction of 2,2-dimethoxy-N-methylethyllamine or 2-methyl-1,3-dioxolane with CS_2 in alkaline media produced two novel dithiocarbamate salts. Subsequent reactions with organotin halides yielded six new complexes: $[SnMe_2\{S_2CNR(R^1)_2\}_2]$ **(1)**, $[Sn(n\text{-}Bu)_2\{S_2CNR(R^1)_2\}_2]$ **(2)**, $[SnPh_2\{S_2CNR(R^1)_2\}_2]$ **(3)**, $[SnMe_2\{S_2CNR(R^2)_2\}_2]$ **(4)**, $[Sn(n\text{-}Bu)_2\{S_2CNR(R^2)_2\}_2]$ **(5)**, $[SnPh_2\{S_2CNR(R^2)_2\}_2]$ **(6)**, where R = methyl, R^1 = $CH_2CH(OMe)_2$, and R^2 = 2-methyl-1,3-dioxolane. All compounds were identified in terms of infrared, ^1H and ^{13}C NMR, and the complexes were also characterized using ^{119}Sn NMR, ^{119}Sn Mössbauer and X-ray crystallography. The biological activity of all derivatives has been screened in terms of IC_{90} and IC_{50} against *Aspergillus flavus*, *Aspergillus niger*, *Aspergillus parasiticus*, *Penicillium citrinum*, *Curvularia senegalensis*, *Staphylococcus aureus*, *Listeria monocytogenes*, *Bacillus cereus*, *Streptococcus sanguinis*, *Escherichia coli*, *Citrobacter freundii*, *Salmonella typhimurium*, and *Pseudomonas aeruginosa* and the results correlated well with a performed study of structure–activity relationship (SAR). Complexes **(3)**, **(5)** and **(6)** displayed the best IC_{90} and IC_{50} in the presence of the fungi, greater than that of miconazole, used as control drug.

1. Introduction

The metal-1,1′-dithiolates comprise one of the most interesting class of complexes, in which three types of anions: xanthates, $ROCS_2^-$, dithiophosphates, $(RO)_2PS_2^-$ and dithiocarbamates, $R_2NCS_2^-$, are the coordinating species [1,2]. Many applications have been found for the latter ligands. Apart from their ability to stabilise metal cations in a variety of oxidation states, well documented in the field of coordination chemistry [3,4], their pharmaceutical properties are noteworthy. They are used to remove excess of copper due to Wilson's disease [5], they are also able to reduce the nephrotoxicity of platinum-based drugs used in chemotherapy [6] and in addition they are used in the treatment of alcoholism [7] and in other clinical applications [8]. In addition they find applications in other fields, for instance in the vulcanization of rubber [9], preparation of pesticides [10], and as precursors for the production of metal sulfide nanoparticles [11–14].

It is also worth to emphasize the varied range of applications and potential use of organotin derivatives, among other metals, as diverse as in agriculture, biology, catalysis, or organic synthesis [15]. As both organotins and dithiocarbamates interact with living cells it is expected an enhanced biological activity by bonding together organotin moieties and dithiocarbamates. Many works have described not only the preparation and characterization of related complexes [16–19] but also their action against tumours, fungi, bacteria, and other microorganisms [1,15,20–23], and other applications [19]. Besides preparing new organotin–dithiocarbamates, investigating their technological applications [24,25] and screening their activity in the presence of some parasites [26,27] we have been interested in the mechanism of action of such complexes in biological media. The number and nature of the organic groups bonded to the metal centre influence the toxicity towards microorganisms, which, in general, decreases in the order $R_3SnX > R_2SnX_2 > RSnX_3$. However, the order of toxicity depends on the microorganism, and varies from strain to strain [28]. It has been proposed that toxicity in the R_3Sn series correlates with total molecule surface (TSA) and hence *n*-propyl-, *n*-butyl-, *n*-pentyl-, phenyl-, and cyclohexyl-substituted tin should be more toxic than ethyl- and

* Corresponding author. Tel.: +55 31 3409 5744; fax: +55 31 3409 5720.
E-mail address: gmlima@ufmg.br (G.M. de Lima).

0223-5234/$ – see front matter © 2012 Elsevier Masson SAS. All rights reserved.
http://dx.doi.org/10.1016/j.ejmech.2012.10.021

methyltin. Moreover, if the toxic effects are intra-cellular, following transport through the cell membrane, a correlation should exist between toxicity and lipophilicity [29]. The effect of organotin-dithiocarbamate and -carboxylate complexes on the cellular activity of some variety of *Candida albicans* revealed that there are no changes in DNA integrity or in the mitochondria function. However, all complexes reduced the ergosterol biosynthesis. Special techniques used for morphological investigations such as scanning electron microscopy (SEM) and transmission electron microscopy (TEM) suggested that the organotin complexes act on the cell membrane, in view of the observed cytoplasm leakage and strong deterioration of the cellular membrane [30].

Following our interest in the chemical, physical and biological properties of metal-based dithiocarbamate complexes herein we describe the synthesis, characterization and the crystallographic authentication of complexes **(1)**–**(6)**. In addition we have screened the biological activity of complexes **(1)**–**(6)** against *Aspergillus flavus*, *Aspergillus niger*, *Aspergillus parasiticus*, *Penicillium citrinum*, *Curvularia senegalensis*, *Staphylococcus aureus*, *Listeria monocytogenes*, *Bacillus cereus*, *Streptococcus sanguinis*, *Escherichia coli*, *Citrobacter freundii*, *Salmonella typhimurium*, and *Pseudomonas aeruginosa*. *Aspergillus* deserves special attention due to the growing number of deaths in consequence of fungal infections in individual who are immunocompromised either from (i) diseases, cancer or AIDS, etc, (ii) the action of immunosuppressive drugs, or (iii) resistance to drugs employed in *Aspergillosis*.

2. Results and discussions

2.1. Chemistry

The new dithiocarbamate sodium salts [Na{S_2CN(Me)R}] R = $CH_2CH(OMe)_2$ **(i)** and (R = 2-methyl-1,3-dioxolane) **(ii)** have been prepared as colourless solids, with yield higher than 90%, by one pot reaction of the appropriate amine with CS_2 in alkaline media. The synthesis of complexes **(1)**–**(6)** have been performed by the chemical reaction of SnR_2Cl_2 with **(i)** or **(ii)** according to Scheme 1.

All complexes have been isolated as colourless, air stable and crystalline solids, with melting points ranging from 80 to 180 °C.

2.2. Infrared results

The infrared spectra of metallic dithiocarbamates normally exhibit strong to moderate signals, allowing important structural outcomes. The vibration studies were focused in three main regions, $\nu_{(N-CS2)}$, $\nu_{(C-S)}$ and $\nu_{(Sn-C)}$. Despite the sensitivity of the Sn–Cl stretching frequency to the coordination number of tin, in **(1)**–**(6)** it was detected in the expected region within 385–318 cm^{-1} [31]. The Sn–C signals that usually occurs in the range of 500–600 cm^{-1}, ν_{asym}(Sn–C), and 530–470 cm^{-1}, ν_{sym}(Sn–C), did not show great changes in **(1)**–**(6)**, if compared to other compounds reported in the literature. The set of bands of the $-CS_2$ fragment are unique since it provides information of the coordination mode of the complexes. If the ligand and metal are bonded in a bidentate form, through both sulphur donor centres, either only one vibration, ν_{asym}, is observed in the *i.r.* spectrum between 1060 and 940 cm^{-1} or this signal splits into two close signals ($\Delta\nu_{asym} < 20\ cm^{-1}$) due to a small asymmetry of the S–C–S fragment. This asymmetry increases in a monodentate bonding scheme, M–S–C=S ($\Delta\nu_{asym} > 20\ cm^{-1}$). The ν_{asym} and ν_{sym} of the C–S bond in the free ligands [Na{S_2CN(Me)$CH_2CH(OMe)_2$}] **(i)** and [Na{S_2CN(Me)R}] **(ii)** (R = 2-methyl-1,3-dioxolane) were observed at 966 and 613 cm^{-1}, 982 and 606 cm^{-1}, respectively. These signals have shifted to higher frequency remaining almost unchanged in **(1)**–**(6)**. Only one signal was detected for the ν_{asym} in the complexes in the range of 950–996 cm^{-1}, indicating mostly a symmetrical bidentate coordination mode [32]. The symmetric vibration of the C–S bond of all complexes ranged from 630 to 420 cm^{-1} [33]. The N–CS bond stretches within 1482–1495 cm^{-1} in the complexes and in the free ligands, **(i)** and **(ii)**, at 1473 and 1474 cm^{-1}, respectively, revealing an increase in the N–C double bond character. The Sn–S bands were detected at low frequencies (250–450 cm^{-1}).

2.3. NMR results

Complexes **(1)**–**(6)** displayed the pattern expected for the ^1H NMR, confirming the formation of the dithiocarbamate. All complexes exhibited an upfield shift for the NCH_2 hydrogen in comparison to the ligands, Table 1.

In the ^{13}C NMR spectra the signal corresponding to $-CS_2$ and those of the carbon bonded to the tin atom were of special interest. The δ (CS_2) signal in the ligands moves to lower frequency in the complexes. A closer relationship between the ^{13}C chemical shift, δ, and ν(N–CS_2) has been described in the literature. Higher values of the stretching frequency of N–C bond indicates a higher double bond character of this interaction, and is related to low values of the $\delta(N^{13}CS_2)$, observed in the NMR, due to a higher electronic density at the carbon atom [34]. The same tendency has been observed in this work. The ν(N–CS_2) locates in higher frequency if compared with sodium salt of the free ligands, and the $\delta(^{13}CS_2)$ is observed in lower field as consequence of an increased π character of the N–C bond upon coordination to Sn(IV) centre, Table 1.

The literature establishes the following range of ^{119}Sn chemical shift for tetra-, penta-, or hexa-coordinated organotin complexes,

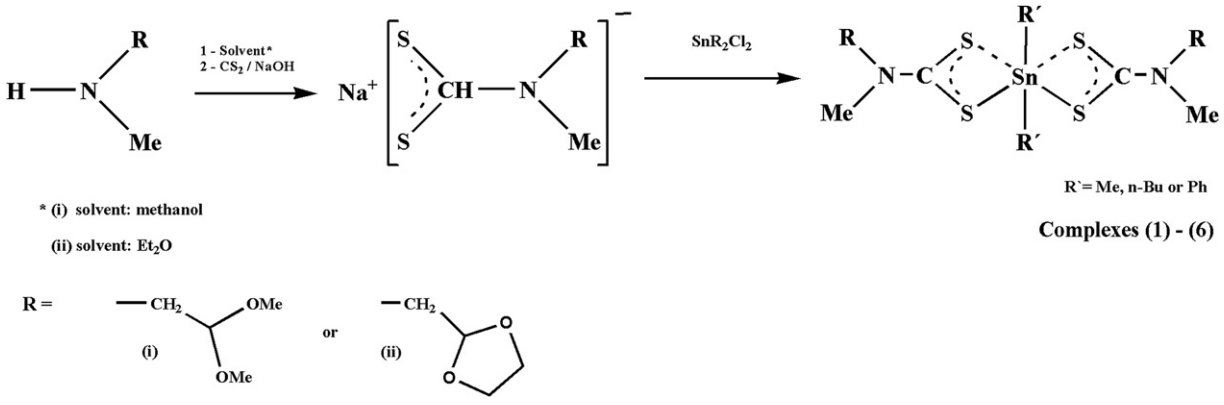

Scheme 1. Synthesis of new dithiocarbamate and their organotin complexes.

Table 1
Selected ^{1}H, ^{13}C and ^{119}Sn NMR and infrared spectroscopic data for compounds **(i)**, **(ii)** and complexes **(1)**–**(6)**.

Compound	$^{1}H/\delta$ (NCH_2)	$^{13}C/\delta$ (NCH_2)	$^{13}C/\delta$ (CS_2)	$\nu_{(N\text{-}CS2)}$	$\nu_{asym(CS2)}$
(i)	4.39–4.42	57.8	214.2	1474	966
$[SnMe_2\{S_2CNR(R^1)\}_2]$ **(1)**	3.90–3.92	58.7	200.8	1485	991
$[Sn(n\text{-}Bu_2\{S_2CNR(R^1)\}_2]$ **(2)**	3.93–3.96	58.7	202.2	1491	979
$[SnPh_2\{S_2CNR(R^1)\}_2]$ **(3)**	3.80–3.83	59.7	203.7	1486	982
(ii)	4.49–4.51	57.3	214.4	1473	982
$[SnMe_2\{S_2CNR(R^2)\}_2]$ **(4)**	3.85–3.90	58.7	201.9	1488	991
$[Sn(n\text{-}Bu)_2\{S_2CNR(R^2)\}_2]$ **(5)**	4.04–4.06	58.8	202.9	1485	995
$[SnPh_2\{S_2CNR(R^2)\}_2]$ **(6)**	3.82–3.96	60.0	201.5	1494	983

δ 200 to −60, δ −90 to −190 and δ −210 to −400 ppm, respectively [35]. However, it must be carefully analysed since apart from coordination number, tin resonance is strongly dependent upon other factors, such as electronegativity of the ligands, temperature and concentration employed in the experiments. In our case, an increase in the coordination number of the tin atom has effected changes in ^{119}Sn δ values in contrast to the starting materials. Nevertheless, in view of the ^{119}Sn NMR results, complexes **(1)**–**(6)** followed the tendency which connects ^{119}Sn chemical shift with coordination number. In solution, the tin centre in complexes **(1)**–**(6)**, remains in a hexa-coordinated environment, Table 2. More informative are the coupling constant ^{1}J (^{119}Sn, ^{13}C) and ^{2}J (^{119}Sn, ^{1}H) obtained in the NMR experiments, which allowed an evaluation of the C–Sn–C angle of the organotin fragment. The literature suggests that ^{1}J and ^{2}J are very sensitive to variation in the coordination number or the C–Sn–C angle. An empirical equation expresses a mathematical relationship between θ and ^{1}J or ^{2}J (^{119}Sn, ^{13}C) coupling constants for methyl–Sn containing complexes [36–38]:

$$|^{1}J(^{119}Sn - {}^{13}C)| = 11.4(\theta) - 875 \quad (1)$$

and

$$(\theta) = (0.0161)\cdot|^{2}J(^{119}Sn, {}^{1}H)|^{2} - 1.32|^{2}J(^{119}Sn, {}^{1}H)|^{2} + 133.4 \quad (2)$$

The interpretation of chemical shifts and coupling constants in solution is generally based on crystal structure data (X-ray), therefore subject to uncertainties arising from solvation and dynamic effects. Equations (1) and (2) provide, with reasonable accuracy a mean of determining the C–Sn–C angle in solution by measuring J coupling parameters. In view of the difficulties of observing ^{2}J (^{119}Sn, ^{1}H) constant, we have used eq. (1) in this work, in spite of its better accuracy observed mostly in methyltin based compounds.

It is observed a decrease of the first order Sn–C coupling constant with coordination number, reflecting changes in θ due to orbital re-hybridization upon complexation [39]. The C–Sn–C angle estimated by eq. (1) agrees with the expected coordination number pointed out by the ^{119}Sn NMR chemical shifts. For those hexa-coordinated complexes it is clear that the structures changes a little in solution or in the solid state, since the C–Sn–C angle measured by X-ray is not too different from that obtained in the ^{119}Sn NMR experiments, Table 2.

2.4. Mössbauer spectroscopic results

The ^{119}Sn-Mössbauer experiments were performed in order to determine the differences in the Sn nuclei on going from organotin starting materials to the complexes. The isomer shift parameters (δ/mm s^{-1}) indicates the presence of s electron density at the tin nuclei, therefore it is a good indication of the hybridization scheme at the tin atom in the complexes. The isomer shift signals for complexes **(1)**–**(6)** were observed at 1.43, 1.58, 1.41, 1.45, 1.57, 1.34 mm s^{-1}, respectively, indicates the presence of Sn(IV) and a pseudo d^2sp^3 hybridization at the tin centre. The non-zero value of the quadrupolar splitting parameters (Δ/mm s^{-1}) indicates deviation from a spherical distribution of charge at the metal atom. For complexes **(1)**–**(6)** we have obtained (Δ/mm s^{-1}) at 3.01, 2.98, 2.78, 2.04, 3.00, 2.57 which is compatible with octahedral geometry [40,41].

2.5. X-ray crystallographic results

Structural determination becomes a key step when the focus of organotin investigations relates to biocide activity, since their performance relies on subtle structural arrangements in solution or in the solid state. The structures of complexes **(1)**–**(6)** have been authenticated by X-ray crystallography [1], Table 3.

In complexes **(1)**–**(6)** there are two asymmetrically coordinating dithiocarbamate ligands, defining a twisted trapezoidal plane described by two distinct pairs of Sn–S bonds. Each one locates at the same side of the molecule, where the similar bonds are *cis* positioned. The short Sn–S bonds vary from 2.5104(9) Å, complex **(3)**, to 2.5324(4) Å in **(6)**, and the longer distances fall in the range of 2.8550(6) in **(6)**, and 3.0045(11) Å, complex **(4)**, Table 4. The longest Sn–S bonds are present in the methyl-containing complexes, 3.0007(7) Å **(1)**, and 3.0045(11) Å, **(4)**. Even though, they are smaller than the sum of the Van der Waals radii of Sn and S (4.0 Å) [42], which suggest a strong covalent character. Therefore the tin cation is surrounded by six donor centres, resulting in a coordination number equal to 6, as observed in previous examples, instead of 4, [43,44]. Another interesting outcome concerns the difference between the short and long Sn–S bonds (Δ_{Sn-S}) in **(1)**–**(6)**, 0.4809 Å, 0.4523 Å and 0.4501 Å, complexes **(1)**–**(3)**, respectively, and 0.4832/0.4891, 0.4071, 0.3226 derivatives **(4)**–**(6)**, accordingly. This asymmetry might results from electronic effects produced by Me, Bu or Ph groups. The electron withdrawing effect of Ph ring

Table 2
^{119}Sn NMR parameters and results and C–Sn–C angle obtained by X-ray crystallography.

Complex[a]	^{119}Sn NMR/δ[b]	C.N.[c]	$^{1}J(^{119}Sn-{}^{13}C)$/Hz	C–Sn–C/°[d]	C C–Sn–C/°[e]
$[SnMe_2\{S_2CNR(R^1)\}_2]$ **(1)**	−334.51	6	757	143.5	136.91(19)
$[Sn(n\text{-}Bu_2\{S_2CNR(R^1)\}_2]$ **(2)**	−339.38	6	605	149.3	138.53(11)
$[SnPh_2\{S_2CNR(R^1)\}_2]$ **(3)**	−498.70	6	777	145.3	139.23(19)
$[SnMe_2\{S_2CNR(R^2)\}_2]$ **(4)**	−335.02	6	749	142.7	137.40(4)
$[Sn(n\text{-}Bu)_2\{S_2CNR(R^2)\}_2]$ **(5)**	−339.58	6	814	148.8	138.29(11)
$[SnPh_2\{S_2CNR(R^2)\}_2]$ **(6)**	−498.45	6	791	146.6	144.92(13)

[a] R = Me; $R^1 = CH_2CH(OMe)_2$ and R^2 = 2-methyl-1,3-dioxolane.
[b] $CDCl_3$ as solvent.
[c] Coordination number at the Sn atom in solution.
[d] Obtained using $|^{1}J(^{119}Sn-{}^{13}C)| = 11.4(\theta) - 875$.
[e] Obtained by X-ray crystallography.

Table 3
Crystallographic data for complexes **(1)**–**(6)**.

Compound	**(1)**	**(2)**	**(3)**	**(4)**	**(5)**	**(6)**
Empirical formula	$C_{14}H_{30}N_2O_4S_4Sn$	$C_{20}H_{42}N_2O_4S_4Sn$	$C_{24}H_{34}N_2O_4S_4Sn$	$C_{14}H_{26}N_2O_4S_4Sn$	$C_{20}H_{38}N_2O_4S_4Sn$	$C_{24}H_{30}N_2O_4S_4Sn$
Formula weight	537.33	621.49	661.46	533.30	617.45	657.43
Temperature, K	293(2)	293(2)	293(2)	543(2)	293(2)	293(2)
Wavelength, Å	0.71073	0.71073	0.71073	0.71073	0.71073	0.71073
Crystal system	Orthorhombic	Monoclinic	Monoclinic	Triclinic	Monoclinic	Monoclinic
Space group	P c c n	C 1 2/c 1	'P 2/c'	P −1	C2/c	C 2/c'
a, Å	9.8722(2)	17.0154(4)	8.9344(5)	9.2515(5)	17.2459(5)	24.9271(10)
b, Å	18.8327(4)	6.9787(2)	6.9234(3)	11.7539(8)	20.1857(5)	6.4287(2)
c, Å	12.2749(2)	23.9908(6)	23.9782(10)	11.7895(6)	8.1113(2)	18.1816(8)
α, °	90	90	90	64.217(6)	90	90
β, °	90	91.160(2)	94.149(4)	77.080(4)	92.677(2)	112.584(5)
γ, °	90	90	90	73.183(5)	90	90
Volume, Å^3	2282.15(8)	2848.21(13)	1479.32(12)	1097.88(11)	2820.63(13)	2690.16(18)
Z	4	4	2	2	4	4
Calculated density, Mg/m^3	1.564	1.449	1.485	1.613	1.454	1.623
Absorption coefficient, mm^{-1}	1.505	1.217	1.177	1.564	1.228	1.294
F(000)	1096	1288	676	540	1272	1336
Crystal size, mm	0.66 × 0.07 × 0.03	0.3175 × 0.16 × 0.1079	0.21 × 0.16 × 0.04	0.28 × 0.17 × 0.06	0.25 × 0.20 × 0.08	0.14 × 0.10 × 0.01
Theta range for data coll., °	2.16–26.37	2.91–26.37	2.29–26.37	1.93–26.37	2.02–26.37	2.39–26.37
Limiting indices	$-12 \le h \le 12$	$-19 \le h \le 21$	$-11 \le h \le 8$	$-11 \le h \le 11$	$-21 \le h \le 21$	$-30 \le h \le 23$
	$-23 \le k \le 23$	$-8 \le k \le 6$	$-8 \le k \le 8$	$-14 \le k \le 11$	$-25 \le k \le 25$	$-7 \le k \le 8$
	$-15 \le l \le 15$	$-29 \le l \le 22$	$-29 \le l \le 29$	$-14 \le l \le 14$	$-10 \le l \le 10$	$-21 \le l \le 22$
Reflections collected	25824	7082	10480	7717	22253	9446
Independent reflections	2342	2919	3033	4492	2887	2749
	[R(int) = 0.0295]	[R(int) = 0.0262]	R(int) = 0.0575]	[R(int) = 0.0351]	[R(int) = 0.0408]	[R(int) = 0.0385]
Reflections obd. (>2 sigma)	2085	2531	2237	3644	2570	2372
Completeness to theta = 26.37	100.0%	99.9%	100.0%	100.0%	100.0%	100.0%
Absorption correction	Multi-scan	Multi-scan	Multi-scan	Multi-scan	Multi-scan	Multi-scan
Refinement method	Full-matrix least-squares on F^2	Full-matrix least-squares on F^2	Full-matrix least-squares on F^2	Full-matrix least-squares on F^2	Full-matrix least-squares on F^2	Full-matrix least-squares on F^2
Data/restraints/parameters	2342/0/114	2919/0/143	3033/0/159	4492/12/226	2887/0/141	2749/0/159
Goodness-of-fit on F^2	1.220	0.984	1.042	1.054	1.073	1.068
Final R indices [I > 2sigma(I)]	R1 = 0.0243	R1 = 0.0232	R1 = 0.0401	R1 = 0.0380	R1 = 0.0219	R1 = 0.0260
	wR2 = 0.0739	wR2 = 0.0483	wR2 = 0.0704	wR2 = 0.0813	wR2 = 0.0502	wR2 = 0.0503
R indices (all data)	R1 = 0.0285	R1 = 0.0298	R1 = 0.0660	R1 = 0.0530	R1 = 0.0279	R1 = 0.0349
	wR2 = 0.0774	wR2 = 0.0498	wR2 = 0.0806	wR2 = 0.0911	wR2 = 0.0540	wR2 = 0.0539
Largest diff. peak and hole, e Å^{-3}	0.438 and −0.406	0.389 and −0.310	0.559 and −0.532	0.547 and −0.582	0.508 and −0.395	0.408 and −0.381
CCDC reference	883619	883618	883621	883620	883622	883617

clearly increases the electronic density at the Sn–S bonds, reducing asymmetry, while the contrary is observed for Me and Bu groups in view of their electron donor nature, producing a greater Δ_{Sn-S}. On butyl-containing complexes **(2)** and **(5)** steric effects might play a key role on this matter too, accounting for the differences in Δ_{Sn-S} on going from methyl- to butyl-bearing derivatives.

Two tin-bonded methyl or butyl groups, with almost similar Sn–C bonds, lie over the weaker Sn ···· S contacts, Figs. 1 and 2. Therefore, the tin centre neighbourhood is best described as being a sort of twisted trapezoidal bipyramid with the four sulphur donor atoms at the equatorial position and two carbons occupying the apical coordination. Considering only the $R_2Sn(S_2CN)_2$ fragment two structural patterns at the tin centre feature the structural arrangements of the diorganotin complexes. Complex **(4)** is formed by two independent crystallographic units where the tin atom is asymmetrically bonded to the S donor centre, as a consequence of

Table 4
Selected bond lengths (Å) and angles (o) for complexes **(1)**–**(6)**.

$[SnMe_2\{S_2CNR(R^1)\}_2]$ **(1)**	$Sn-S^1$	2.5198(7)	Sn–C	2.116(3)	$C-S^1$	1.741(2)
	$Sn-S^2$	3.0007(7)	C^1-N^1	1.332(3)	$C-S^2$	1.692(3)
	S^2-Sn-S^2	149.78(3)	S^1-Sn-S^1	82.00(3)	C^7-Sn-C^7	136.89(17)
$[Sn(n\text{-}Bu)_2\{S_2CNR(R^1)\}_2]$ **(2)**	$Sn-S^1$	–	Sn–C	2.136(2)	$C-S^1$	1.632(3)
	$Sn-S^2$	2.5278(5)	C^1-N^1	1.334(2)	$C-S^2$	1.741(3)
	S^1-Sn-S^1	146.02(2)	S^2-Sn-S^2	84.80(2)	C^7-Sn-C^7	138.53(11)
$[Sn(n\text{-}Ph)_2\{S_2CNR(R^1)_2\}_2]$ **(3)**	$Sn-S^1$	2.5104(9)	$Sn-C^7$	2.118(3)	C^1-S^1	1.738(3)
	$Sn-S^2$	2.9605(9)	C^1-N^1	1.343(4)	C^1-S^2	1.682(3)
	$S^{1i}-Sn-S^1$	84.66(4)	$S^{2i}-Sn-S^2$	145.73(4)	$C^{7i}-Sn-C^7$	139.23(19)
$[SnMe_2\{S_2CNR(R^2)\}_2]$ **(4)**	$Sn-S^1$	2.5156(11)	$Sn-C^{13}$	2.109(4)	C^1-S^1	1.734(4)
	$Sn-S^2$	2.9988(12)	$Sn-C^{14}$	2.110(4)	C^1-S^2	1.685(4)
	$Sn-S^3$	2.5154(11)	C^1-N^1	1.336(5)	C^7-S^3	1.743(4)
	$Sn-S^4$	3.0045(11)	C^7-N^2	1.331(5)	C^7-S^4	1.684(4)
	S^1-Sn-S^3	82.31(3)	S^2-Sn-S^4	149.48(3)	$C^{13}-Sn-C^{14}$	136.14(19)
$[Sn(n\text{-}Bu)_2\{S_2CNR(R^2)\}]$ **(5)**	$Sn-S^1$	2.9392(5)	$Sn-C^1$	2.135(2)	C^5-S^1	1.690(2)
	$Sn-S^2$	2.5321(5)	C^5-N^1	1.340(2)	C^5-S^2	1.743(2)
	S^1-Sn-S^1	145.31(2)	S^2-Sn-S^2	84.06(2)	C^1-Sn-C^1	138.29(11)
$[SnPh_2\{S_2CNR(R^2)\}_2]$ **(6)**	$Sn-S^1$	2.5324(4)	$Sn-C^1$	2.152(2)	C^7-S^1	1.752(2)
	$Sn-S^2$	2.8550(6)	C^7-N^1	1.328(3)	C^7-S^2	1.692(2)
	S^1-Sn-S^1	86.12(3)	S^2-Sn-S^3	141.60(3)	C^1-Sn-C^1	144.92(13)

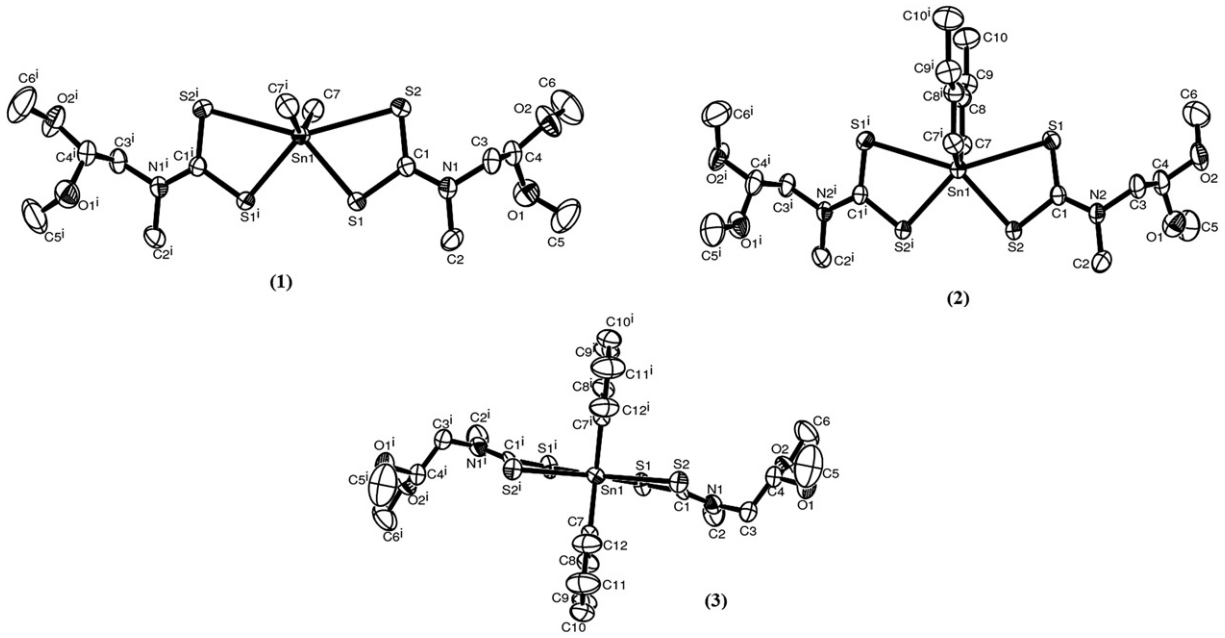

Fig. 1. Structure of the complexes $[SnMe_2\{S_2CNR(R^1)_2\}_2]$ **(1)**, $[Sn(n\text{-}Bu)_2\{S_2CNR(R^1)_2\}_2]$ **(2)**, $[SnPh_2\{S_2CNR(R^1)_2\}_2]$ **(3)**, where R = methyl and $R^1 = CH_2CH(OMe)_2$.

the coordination mode and π-electron density distribution at the $-CS_2$ groups. All four S atoms, in **(1)**–**(6)** situate at the same plane. The short S–Sn–S angle situates between 82.00(3)° in **(1)**, and 86.12(3)° in **(6)**, agreeing with literature data [22,23]. Complex **(1)**, displayed the smaller C–Sn–C angle, 136.89(17)° in contrast to **(6)**, 144.92(13)°, however it is in the range observed in the literature [1,19,23–30]. Solvation process produces little structural variation in the C–Sn–C angles in solution, as pointed out by the $J_{(Sn-^{13}C)}$ coupling constants. The S_{short}–Sn–S_{short} angles of complexes **(1)**–**(6)** ranged from 82.00(3)° in complex **(1)** to 86.12(3)° in **(6)**, and the S_{long}–Sn–S_{long} varied from 141.60(3)° in **(6)** to 149.78(3)° in **(1)**, Table 4.

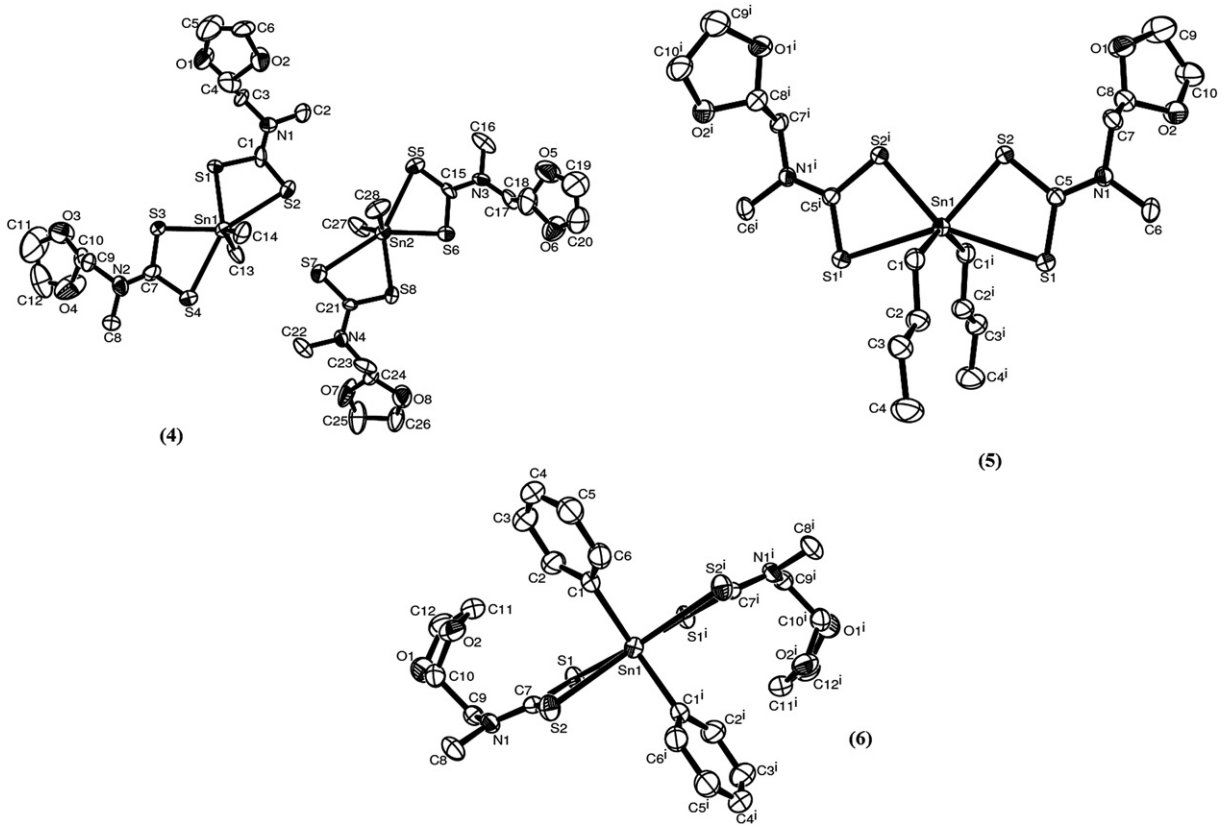

Fig. 2. Structure of the complexes $[SnMe_2\{S_2CNR(R^2)_2\}_2]$ **(4)**, $[Sn(n\text{-}Bu)_2\{S_2CNR(R^2)_2\}_2]$ **(5)**, $[SnPh_2\{S_2CNR(R^2)_2\}_2]$ **(6)**, where R = methyl and R^2 = 2-methyl-1,3-dioxolane.

2.6. Biocide assay results

Most of the results concerning the organotins interaction with living cells are obtained using in agar or other diffusion media [18,21,23,44]. Interactions of the complexes with the media in diffusion tests might influence the results, frustrating reliable outcomes. In this work the biocide assays were performed in terms of inhibitory concentrations, which are more consistent. The organotin dithiocarbamates have been used in a concentration of 250 μg mL^{-1}, in an antimicrobial pre-screening against *A. flavus*, *A. niger*, *A. parasiticus*, *P. citrinum*, *C. senegalensis*, *S. aureus*, *L. monocytogenes*, *B. cereus*, *S. sanguinis*, *E. coli*, *C. freundii*, *S. typhimurium*, *P. aeruginosa*, according to a pre-established protocol [45]. Experiments of IC_{90} and IC_{50} were only performed for those complexes that displayed 100% inhibition growth of the studied microorganism in a concentration of 250 μg mL^{-1}. In spite of the poor activity against *C. senegalensis* intense antifungal activity was found in the presence of filamentous fungus such as *A. flavus*, *A. niger*, *A. parasiticus* and *P. citrinum*, therefore we conclude that the complexes are inactive against the other microorganisms. Only the bacteria, *S. aureus* and *E. coli*, had the growth affected by the presence of complexes **(1)**–**(6)**.

We have observed the following tendency of the complexes concerning the inhibition of *A. flavus*, (i) IC_{90}: **(6)** < **(3)** < miconazole < **(5)** < **(1)** < **(2)** < **(4)** < nystatin << sodium salts; (ii) IC_{50}: **(6)**, **(3)** < **(1)**, **(4)**, < miconazole < **(5)** < nystatin < **(2)** << sodium salts. Complexes **(6)**, **(3)** and **(1)** were more active than miconazole, Table 5.

The complexes had the following behaviour in the presence of *A. niger*, IC_{90}: miconazole < **(3)** < **(5)** < **(6)** < nystatin < the others complexes << sodium salts; (ii) IC_{50}: miconazole < **(3)** < **(5)** < **(6)** < nystatin < the other complexes << sodium salts. We observe similar activity of **(3)** and **(5)** and lesser of **(6)** comparing to miconazole.

The organotin derivatives influenced the growth of *A. parasiticus* as follows, IC_{90}: miconazole < **(3)** < **(6)** < **(5)** < nystatin < the other complexes << sodium salts; (ii) IC_{50}: miconazole < **(3)**, **(6)** < **(5)** < nystatin < the other complexes << sodium salts. In this case miconazole is much more active than **(3)**, **(5)** and **(6)**.

Finally, compounds **(1)**–**(6)** exhibited the following behaviour against the colony of *P. citrinum* displaying IC_{90}: **(3)** < **(5)** < miconazole < **(6)** < **(1)**, **(4)** < nystatin < **(2)** << sodium salts; (ii) IC_{50}: **(3)** < **(6)** < **(5)** < **(2)** < miconazole < **(4)**, **(1)** < nystatin << sodium salts. In here it was observed that complex **(3)** is far more active if compared to the other complexes and miconazole, Table 5.

In general complexes **(1)**–**(6)** interact better with filamentous fungus rather than yeasts, revealing higher selectivity if compared with miconazole, which was effective against all microorganisms. On the other hand the sodium salts were inactive towards the studied fungi. The toxicity of the organotin dithiocarbamates depends on the nature of the organic group attached to Sn(II) centre. Those complexes with R = Ph, $[SnPh_2\{S_2CNR(R^1)\}_2]$ $\{R^1 = CH_2CH(OMe)_2\}$ **(3)**, $[SnPh_2\{S_2CNR(R^2)\}_2]$ $\{R^2$ = 2-methyl-1,3-dioxolane$\}$ **(6)** displayed the best activities in terms of IC_{90} and IC_{50} comparing to the other organic groups, followed by $[Sn(n\text{-}Bu)_2\{S_2CNR(R^2)\}_2]$ $\{R^2$ = 2-methyl-1,3-dioxolane$\}$ **(5)**.

The best results towards *S. aureus* and *E. Coli* were observed for $SnMe_2\{S_2CNR(R^2)_2\}_2]$ **(4)**, $[Sn(n\text{-}Bu)_2\{S_2CNR(R^2)_2\}_2]$ **(5)**, $[SnPh_2\{S_2CNR(R^2)_2\}_2]$ **(6)**. The dithiocarbamates displaying $R^1 = CH_2CH(OMe)_2$ were less active than R^2 = 2-methyl-1,3-dioxolane towards the tested bacteria. Those complexes containing the Bu_2Sn- and Ph_2Sn-fragments displayed better activity towards *E. coli*, and Me_2Sn-containing moiety was effective against *S. aureus*, Table 5.

2.7. Relation between the structure of the complexes and their biologic activity

In fungi, ergosterol is a key molecule for cell integrity, regulating fluidity, permeability and indirectly modulating the activity and distribution of membrane-associated proteins, including enzymes and ion channels, hence controlling physiological events which are responsible for maintaining the life cycle. Therefore, the enzymes participating of ergosterol biosynthesis are potential targets for development of fungicide drugs. Among the enzymes, stands out the sterol 14α-demethylase, the target of azoles derivatives, such as itraconazole, fluconazole and voriconazole, etc [46–48]. In previous work we have observed organotin dithiocarbonates and carboxilates decrease the biosynthesis of ergosterol [30,49].

To study the structure–activity relationship (SAR), we have used theoretical calculations to obtain structural and stereo-electronic parameters that support promising mechanisms related to the transport of each compound across the cell membranes, revealing possible interactions with biological macromolecules, for instance enzymes. Therefore, we have calculated the energies of the HOMO and LUMO orbitals, the lipophilicity (LogP), dipole moment, surface area and volume of complexes **(1)**–**(6)**, Table 6.

The difference between the energies of HOMO and LUMO (HOMO–LUMO gap) shows the stability and reactivity of the molecules, pointing out in the complexes possible biological receptors such as electron rich or electron deficient regions [50–52]. The lipophilic nature of the complexes can be evaluated by the logarithm of the partition coefficient (LogP), that indicates the ability of the molecule to overcome biological barriers and move into different biophases [53].

Table 5
Inhibition concentration of 90% (IC_{90}) and 50% (IC_{50}) (μmol L^{-1}) for the organotin complexes.

Complexes	*A. flavus*		*A. niger*		*A. parasiticus*		*P. citrinum*		*S. aureus*	*E. coli*
	IC_{90}	IC_{50}	IC_{90}	IC_{50}	IC_{90}	IC_{50}	IC_{90}	IC_{50}	IC_{50}	IC_{50}
$[SnMe_2\{S_2CNR(R^1)\}_2]$ **(1)**	58.2	<0.22	232.6	58.2	465.2	232.6	232.6	58.2	232.6	47.3
$[Sn(n\text{-}Bu_2\{S_2CNR(R^1)\}_2]$ **(2)**	201.2	6.29	201.2	25.14	402.3	100.6	402.3	25.1	201.2	201.2
$[SnPh_2\{S_2CNR(R^1)\}_2]$ **(3)**	0.369	<0.18	2.95	0.369	11.8	2.95	1.48	0.369	94.5	116.3
$[SnMe_2\{S_2CNR(R^2)\}_2]$ **(4)**	234.4	<0.22	234.4	29.3	468.8	117.2	234.4	58.6	14.7	47.5
$[Sn(n\text{-}Bu)_2\{S_2CNR(R^2)\}_2]$ **(5)**	25.3	0.791	3.16	1.58	50.6	25.3	50.6	12.6	50.6	12.7
$[SnPh_2\{S_2CNR(R^2)\}_2]$ **(6)**	0.186	<0.18	23.8	1.48	23.8	2.97	95.1	11.9	190.2	14.7
$[Na\{S_2CN(Me)R^1\}]$	1150.9	2.25	575.4	143.8	1150.9	575.4	575.4	287.7	–	–
$[Na\{S_2CN(Me)R^2\}]$	11623.4	1452.0	5811.7	2905.0	11623.0	5811.7	11623.0	2905.0	–	–
Nystatin	269.9	4.22	67.49	16.87	269.9	67.49	>269.9	269.9	–	–
Miconazole nitrate	4.08	<0.25	2.04	<0.25	1.02	<0.255	65.23	32.61	–	–
Chloramphenicol	–	–	–	–	–	–	–	–	<0.997	–
Ampicillin	–	–	–	–	–	–	–	–	–	1.18

R = Me; $R^1 = CH_2CH(OMe)_2$ and R^2 = 2-methyl-1,3-dioxolane.

Table 6
- IC_{50} values, stereo-electronic properties calculated for complexes **(1)**–**(6)**.

Complex	E_{HOMO} (eV)	E_{LUMO} (eV)	ΔE (eV)	μ (D)	S. A. (Å^2)[a]	V (Å^3)	Log P	Charge (e.u.)[b]		
								Sn	S	S
$[SnMe_2\{S_2CNR(R^1)\}_2]$ **(1)**	−5.815	−0.827	4.988	2.347	664.15	413.08	5.65	0.7516	−0.1168	−0.2528
$[Sn(n\text{-}Bu_2\{S_2CNR(R^1)\}_2]$ **(2)**	−5.826	−0.811	5.015	0.163	848.76	514.92	8.20	0.7090	−0.2531	−0.1293
$[SnPh_2\{S_2CNR(R^1)\}_2]$ **(3)**	−5.701	−0.781	4.920	0.390	816.02	522.8	8.01	0.6932	−0.2258	−0.1212
									−0.1114	−0.2502
$[SnMe_2\{S_2CNR(R^2)\}_2]$ **(4)**	−5.791	−0.756	5.034	5.037	610.78	390.37	5.3	0.7073	−0.1195	−0.2448
$[Sn(n\text{-}Bu)_2\{S_2CNR(R^2)\}_2]$ **(5)**	−5.733	−0.746	4.988	4.250	794.7	492.28	7.84	0.6898	−0.1380	−0.2349
$[SnPh_2\{S_2CNR(R^2)\}_2]$ **(6)**	−5.644	−0.748	4.895	4.762	762.99	500.28	7.65	0.6339	−0.1966	−0.1546

R = Me; $R^1 = CH_2CH(OMe)_2$ and R^2 = 2-methyl-1,3-dioxolane.
[a] S.A. = surface area.
[b] e.u. = electrostatic unit.

Similar values of surface area, molecular volume and LogP are observed in each pair of derivatives: $[Sn(n\text{-}Bu)_2\{S_2CNMe(R^1)_2\}_2]$ **(2)** and $[SnPh_2\{S_2CNMe(R^1)_2\}_2]$ **(3)**; $[Sn(n\text{-}Bu)_2\{S_2CNMe(R^2)_2\}_2]$ **(5)** and $[SnPh_2\{S_2CNMe(R^2)_2\}_2]$ **(6)**; $[SnMe_2\{S_2CNMe(R^1)_2\}_2]$ **(1)** and $[SnMe_2\{S_2CNMe(R^2)_2\}_2]$ **(4)**, {$R^1 = CH_2CH(OMe)_2$, R^2 = 2-methyl-1,3-dioxolane}. The higher values of the steric properties and LogP are found for **(2)**/**(3)**, and then for **(5)**/**(6)**. These theoretical parameters correlate well with the experimental results since complex **(3)** is the most active against all fungi, studied in this work, followed by **(5)** and **(6)**. Unfortunately complex **(2)** was inactive. Some connection have also been observed between experiments and HOMO and LUMO calculation. Although little differences are detected in the atomic participation in the formation of frontier orbitals in the complexes, the main contribution to HOMO arises from sulphur orbitals, while the LUMO involves sulphur, carbon and nitrogen orbitals, of the dithiocarbamates, Fig. 3.

In spite of the energies of the frontier orbitals in **(1)**–**(6)** are quite close, Table 6, compounds **(3)** and **(6)** showed less negative values for the energy of the HOMO and smaller HOMO/LUMO gap (ΔE), suggesting higher reactivity in the biologic media compared to the other complexes. Furthermore, complexes **(3)**, **(5)** and **(6)** display the smallest differences between the sulphur charges and smaller asymmetry in the C–S bonds, Table 6, implying in greater lipophilicity.

The reasonable agreement of theoretical calculations and experiments leads us to suppose that biocide activity of **(1)**–**(6)** strongly depends upon their lipophilicity and steric effects. The lipid-solubility of organotin complexes might results from weak interactions with amino-acids, proteins, nucleosides, enzymes, carbohydrates, etc, present in the cell membrane. The influence of steric parameters may suggest an enzyme–organotin complex interaction (*e.g.* in a lock–key fashion), validating our previous results pointing out the ergosterol biosynthesis inhibition as mode of action of organotin dithiocarbamates [30,49]. However, in sight of the subtle structural features revealed by the structure–activity relationship (SAR) study, more findings are necessary to disregard other possible mechanisms.

Finally, we found no correlation of the biocide activity of the organotin dithiocarbamate complexes with their magnetic moment, Table 6.

Complexes **(3)**, **(5)** and **(6)** might represent a new class of drug to be employed alone or in combination with others in current use as new formulations for fungi diseases, especially to overcome drug resistance, the challenge of next decades. In spite of all controversy around the toxicity of organotin towards mammals and other superior species it is possible that some of their complexes are not as hazardous as organotin halides. However, the mechanism related to the interactions of organotin with mammals requires a better understanding.

3. Experimental

3.1. Chemistry

3.1.1. Materials and instruments

All starting materials were purchased from Aldrich, Merck or Synth and used as received. NMR spectra were recorded at 400 MHz using a Bruker DPX-400 spectrometer equipped with an 89 mm wide-bore magnet. ^{1}H and ^{13}C shifts are reported relative to $SiMe_4$ and ^{119}Sn shifts relative to $SnMe_4$. The infrared spectra were recorded with samples pressed as KBr pellets on a Perkin–Elmer GX FT-IR spectrometer in the range of 4000–200 cm^{-1}. Carbon, hydrogen and nitrogen analysis were performed on a Perkin–Elmer PE-2400 CHN-analysis using tin sample-tubes. ^{119}Sn Mössbauer spectra were run in standard equipment at liquid nitrogen temperature using a $BaSnO_3$ source kept at room temperature. Intensity data for the X-ray study were collected at 293(2) K on a Xcalibur, Atlas, Gemini, Kα/Mo (λ = 0.7107 Å). Data collection, reduction and cell refinement were performed using the CrysAlis RED program [54]. The structures were solved employing the SHELXS-97 [55] and refined with SHELXL-97 [56]. Further details are given in Table 1. All non-H atoms were refined anisotropic. The H atoms were refined with fixed individual displacement parameters [Uiso (H)Z1.2 Ueq (C)] using the SHELXL riding model. The program ORTEP-3 for Windows [57] was used in the preparation of Figs. 1 and 2.

3.2. The structure–activity relationship (SAR)

Geometry optimization and frequency calculations of all compounds studied in this work were performed at the Density Functional Theory level [58], employing the hybrid B3LYP [59,60] exchange-correlation functional and using the 6-31G(d) all electron basis set [61,62] for all atoms. The tin atom was treated using the LANL2DZ pseudopotential for the core electrons and its associated double-zeta basis set for the valence electrons [63]. All properties involved in the SAR studies were obtained for the optimized structures. The quantum mechanical calculations were performed using the Gaussian 03 program [64]. The molecular surface area, molecular volume and octanol–water partition coefficients (logP) of all species were computed using the MarvinView program [65].

3.3. Syntheses

3.3.1. $[Na\{S_2CN(Me)R\}]$ {$R = CH_2CH(OMe)_2$} ***(i)***

A round-bottom flask (250 mL) was charged with 2,2-dimethoxy-N-methylethyllamine (20.0 g − 167.8 mmol), methanol (100 mL), and cooled in an ice/NaCl bath. After 10 min stirring, carbon disulfide (10.1 mL − 167.8 mmol) was slowly added to the

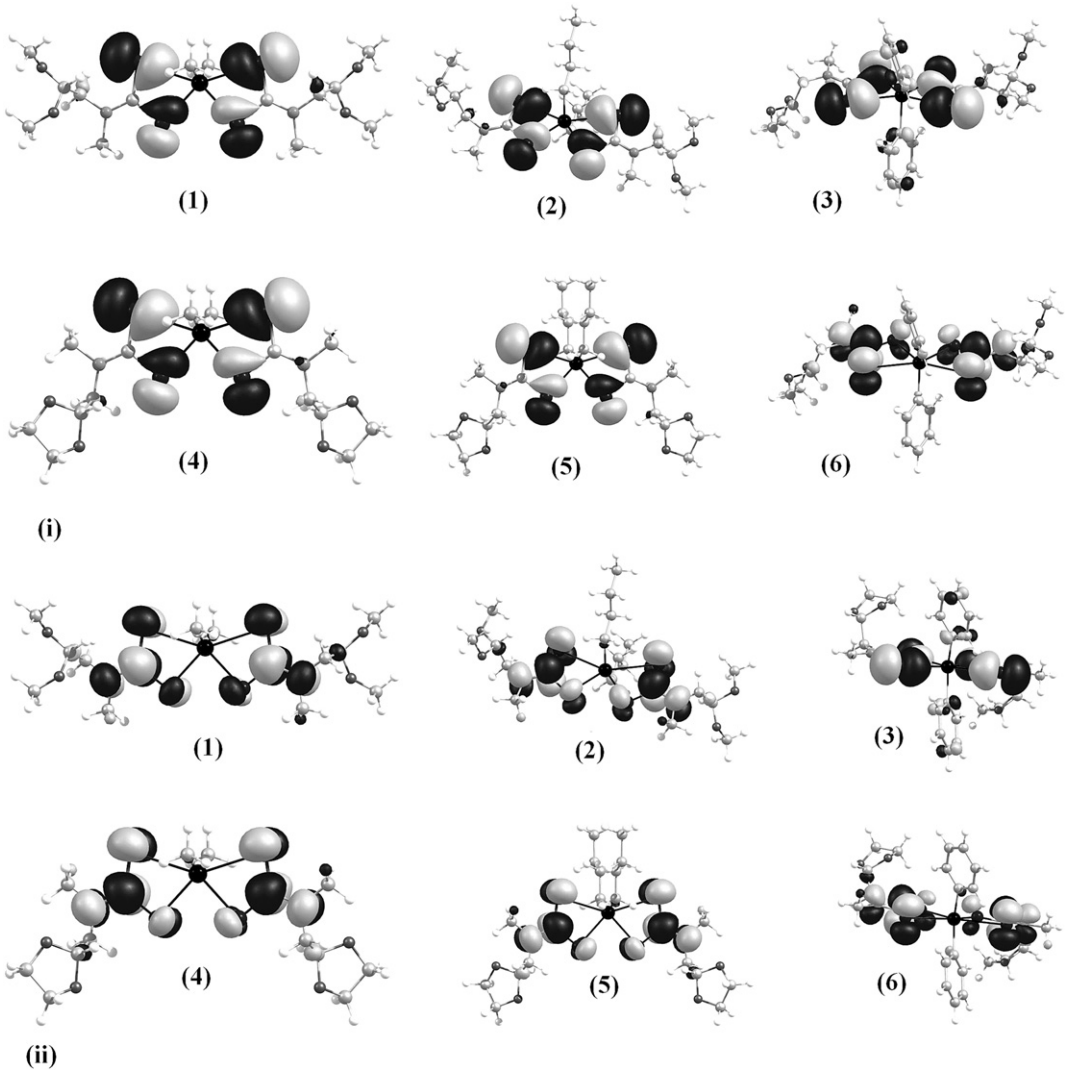

Fig. 3. The HOMO **(i)** and LUMO **(ii)** plots for complexes **(1)**–**(6)**.

round-bottom flask, and a colour change from colourless to pale-yellow was observed. NaOH (6.71 g – 167.8 mmol), dissolved in a minimal amount of water was added, forming, almost immediately, a white solid. The reaction mixture was stirred for further 1 h at ambient temperature and then the solid was isolated by filtration, washed with toluene and re-crystallized in a mixture of CH_2Cl_2/toluene (4:1). Yield 97%. Mp 83.9–85.2 °C. IR (cm^{-1}, KBr): 1474 (ν_{N-CS}); 966 {$\nu_{asym(C-S)}$}; 613 {$\nu_{sym(C-S)}$}. ^1H NMR (^1H NMR, d_4-methanol): 5.08–5.13 (CH); 4.39–4.42 (NCH_3); 3.74 (NCH_3); 3.64 (OCH_3). ^{13}C NMR (^{13}C NMR, d_4-methanol): 214.2 (CS_2); 104.5 (CH); 57.8 (NCH_2); 54.2 (OCH_3); 44.1 (NCH_3). Analysis for $C_6H_{12}NO_2S_2Na$: found (calc.) 33.15 (33.18); 5.51 (5.57); 6.41 (6.45).

3.3.2. Synthesis of [Na{$S_2CN(Me)R$}] (R = 2-methyl-1,3-dioxolane) *(ii)*

Similarly prepared in methanol (100 mL) using (1,3-dioxolane-2-methyl)-N-methylamine (5.0 g – 42.7 mmol); CS_2 (2.58 mL – 42.7 mmol), NaOH (10.0 g – 42.7 mmol). Yield 93%. Mp 46.7–49.1 °C. IR (cm^{-1}, KBr): 1473 (ν_{N-CS}); 982 {$\nu_{asym(C-S)}$}; 606 {$\nu_{sym(C-S)}$}. ^1H NMR (δ, d_4-methanol): 5.54 – 5.49 (OCHO). 4.51–4.49 (NCH_2); 4.23–4.09 (OCH_2); 3.19 (NCH_3). ^{13}C NMR (δ, d_4-methanol): 214.4 (CS_2); 103.1 (OCHO); 65.8 (OCH_2); 59.3 (NCH_2); 45.0 (NCH_3). Analysis for $C_6H_{10}NO_2S_2Na$: found (calc.) 32.97 (33.49); 4.62 (4.68); 6.26 (6.51).

3.3.3. Synthesis of [$SnMe_2${$S_2CN(Me)R$}$_2$] {R = $CH_2CH(OMe)_2$} *(1)*

To a round-bottom flask (125 mL) containing [$SnMe_2Cl_2$] (1 g – 4.6 mmol) in ethanol (20 mL) was added [Na{$S_2CN(Me)R$}], R = $CH_2CH(OMe)_2$ (2.00 g – 9.2 mmol), previously dissolved in the same solvent. After stirring for 24 h, the white precipitate was filtered and washed with hot water and ethanol. The solid obtained was re-crystallized in a 4:1 mixture of CH_2Cl_2/methanol. Colourless X-ray quality crystals were obtained by evaporation of the solvent at room temperature. Yield 85%. Mp 116.9–118.1 °C. IR (cm^{-1}, KBr): 1485 (ν_{N-CS}); 991 {$\nu_{asym(C-S)}$}; 644 {$\nu_{sym(C-S)}$}; 372 {$\nu_{asym(S-Sn)}$}; 335 {$\nu_{sym(S-Sn)}$}. ^1H NMR (δ, $CDCl_3$): 4.73 (CH); 3.92–3.90 (NCH_2); 3.44–3.41 (OCH_3) and (NCH_3); 1.46 (Sn–CH_3). ^{13}C NMR (δ, $CDCl_3$): 200.8 (CS_2); 102.3 (CH); 58.7 (NCH_2); 55.3 (OCH_3); 44.8 (Sn–CH_3). ^{119}Sn NMR (δ, $CDCl_3$): –334.5 {$^1J(^{119}Sn-^{13}C)$ = 757 Hz, $^2J(^{119}Sn-^1H)$ = 81.1 Hz}. δ (mm s^{-1}): 1.43; Δ (mm s^{-1}): 3.01. Analysis for $C_{14}H_{30}N_2O_4S_4Sn$: found (calc.) 31.24 (31.29); 5.61 (5.63); 5.17 (5.21).

3.3.4. Synthesis of [$Sn(n\text{-}Bu)_2${$S_2CN(Me)R$}$_2$] {R = $CH_2CH(OMe)_2$} *(2)*

Prepared in a similar manner using [$Sn(n\text{-}Bu)_2Cl_2$] (1.39 g – 4.6 mmol) and [Na{$S_2CN(Me)R$}], R = $CH_2CH(OMe)_2$ (2.00 g – 9.2 mmol). Re-crystallization in a mixture of CH_2Cl_2/toluene (5:1) afforded X-ray quality crystals of complex **(2)**. Yield 37%. Mp 118.2–119.2 °C. IR (cm^{-1}, KBr): 1491 (ν_{N-CS}); 979 {$\nu_{asym(C-S)}$}; 613 {$\nu_{sym(C-$

S)}; 370 {$\nu_{asym(S-Sn)}$}; 324 {$\nu_{sym(S-Sn)}$}. ^{1}H NMR (δ, $CDCl_3$): 4.78–4.73 (C*H*); 3.96–3.93 (NCH_2); 3.47–3.43 (OCH_3) and (NCH_3); 2.1–0.9 Sn–C_4H_9. ^{13}C NMR (δ, $CDCl_3$): 202.2 (CS_2); 102.5 (*C*H); 58.7 (NCH_2); 55.4 (OCH_3); 44.6 (NCH_3); 34.3–13.8 (Sn–C_4H_9). ^{119}Sn NMR (δ, $CDCl_3$): −339 {$^1J(^{119}Sn-^{13}C)$ = 605 Hz}. δ (mm s^{-1}): 1.58; Δ (mm s^{-1}): 2.98. Analysis for $C_{20}H_{42}N_2O_4S_4Sn$: found (calc.) 38.25 (38.66); 6.76 (6.81); 4.46 (4.51).

3.3.5. Synthesis of [$SnPh_2\{S_2CN(Me)R\}_2$] {R = $CH_2CH(OMe)_2$} **(3)**

It was prepared similarly employing: ethanol (20 mL); [$SnPh_2Cl_2$] (1 g − 4.6 mmol), [Na{$S_2CN(Me)R$}], R = $CH_2CH(OMe)_2$ (2.00 g − 9.2 mmol). X-ray quality crystals were grown in CH_2Cl_2/ethanol solution of complex **(3)**. Yield 56%. Mp 176.9–178.4 °C. IR (cm^{-1}, KBr): 1486 (ν_{N-CS}); 982 {$\nu_{asym(C-S)}$}; 608 {$\nu_{sym(C-S)}$}; 456 {$\nu_{asym(S-Sn)}$}; 418 {$\nu_{sym(S-Sn)}$}. ^{1}H NMR (δ, $CDCl_3$): 7.90–7.33 (Sn–C_6H_5); 4.73–4.70 (C*H*); 3.83–3.80 (NCH_2); 3.38 (OCH_3) and (NCH_3). ^{13}C NMR (δ, $CDCl_3$): 203.8 (CS_2); 151–127.5 (Sn–C_6H_5); 102.1 (C*H*); 59.7 (NCH_2); 55.9 (OCH_3); 45.7 (NCH_3). ^{119}Sn NMR (δ, $CDCl_3$): −498.7 {$^1J(^{119}Sn-^{13}C)$ = 777 Hz and $^2J(^{119}Sn-^1H)$ = 82.6 Hz}. δ (mm s^{-1}): 1.41; Δ (mm s^{-1}): 2.78. Analysis for $C_{24}H_{34}N_2O_4S_4Sn$: found (calc.) 43.49 (43.58); 5.11 (5.18); 4.15 (4.24).

3.3.6. Synthesis of [$SnMe_2\{S_2CN(Me)R\}_2$] (R = 2-methyl-1,3-dioxolane) **(4)**

It was similarly prepared using [$SnMe_2Cl_2$] (1.02 g, 4.6 mmol) and [Na{$S_2CN(Me)R$}] (R = 2-methyl-1,3-dioxolane) (2.0 g, 9.2 mmol). The white solid isolated by filtration was re-crystallized in a mixture of $CHCl_3$/toluene (5:1) affording X-ray quality crystals. Yield 78%. Mp 134.5–136.3 °C. IR (cm^{-1}, KBr): 1488 (ν_{N-CS}); 991 {$\nu_{asym(C-S)}$}; 609 {$\nu_{sym(C-S)}$}. ^{1}H NMR (δ, $CDCl_3$): 4.00–3.93 (OCH_2); 3.90–3.85 (NCH_2 and OC*H*O); 3.44 (NCH_3); 1.46 (Sn–CH_3); ^{13}C NMR (δ, $CDCl_3$): 201.9 (CS_2); 100.9 (OCHO); 64.9 (OCH_2); 58.7 (NCH_2); 14 (Sn–*C*H_3). ^{119}Sn NMR (δ, $CDCl_3$): −335.1 {$^1J(^{119}Sn-^{13}C)$ = 749 Hz, $^2J(^{119}Sn-^1H)$ = 83.2 Hz}. δ (mm s^{-1}): 1.41; Δ (mm s^{-1}): 2.78. Analysis for $C_{14}H_{26}N_2O_4S_4Sn$: found (calc.) 31.44 (31.54); 5.03 (4.92); 5.17 (5.25).

3.3.7. Synthesis of [$Sn(n\text{-}Bu)_2\{S_2CN(Me)R_2\}_2$] (R = 2-methyl-1,3-dioxolane) **(5)**

It was similarly prepared using [$Sn(n\text{-}Bu)_2Cl_2$] (1.41 g, 4.6 mmol) and [Na{$S_2CN(Me)R$}] (R = 2-methyl-1,3-dioxolane) (2.0 g, 9.2 mmol). The white solid isolated by filtration was re-crystallized in a mixture of $CHCl_3$/toluene (4:1) affording X-ray quality crystals. Yield 95%. Mp 69.1–71.1 °C. IR (cm^{-1}, KBr): 1486 (ν_{N-CS}); 982 {$\nu_{asym(C-S)}$}; 608 {$\nu_{sym(C-S)}$}; 456 {$\nu_{asym(S-Sn)}$}; 418 {$\nu_{sym(S-Sn)}$}. ^{1}H NMR (δ, $CDCl_3$): 5.25–5.20 (OC*H*O); 4.10 (NCH_2); 4.00–3.50(OCH_2); 3.49 (NCH_3); 2.17–0.89 (Sn–C_4H_7). ^{13}C NMR (δ, $CDCl_3$): 202.9 (CS_2); 101.3 (OCHO); 64.9 (OCH_2); 58.8 (NCH_2); 44.2 (NCH_3); 34.2–13.8 (Sn–C_4H_7). ^{119}Sn NMR (δ, $CDCl_3$): −339.6 {$^1J(^{119}Sn-^{13}C)$ = 814 Hz}. δ (mm s^{-1}): 1.41; Δ (mm s^{-1}): 2.78. Analysis for $C_{20}H_{38}N_2O_4S_4Sn$: found (calc.) 38.78 (38.91); 6.43 (6.20); 4.49 (4.54).

3.3.8. Synthesis of [$SnPh_2\{S_2CN(Me)R_2\}_2$] (R = 2-methyl-1,3-dioxolane) **(6)**

Synthesized accordingly using [$SnPh_2Cl_2$] (1.59 g, 4.6 mmol) and [Na{$S_2CN(Me)R$}] (R = 2-methyl-1,3-dioxolane) (2.0 g, 9.2 mmol). The white solid isolated by filtration was re-crystallized in a mixture of CH_2Cl_2/ethanol (4:1) rendering crystals for X-ray quality experiments. Yield 46%. Mp 132.9–134.1 °C. IR (cm^{-1}, KBr): 1486 (ν_{N-CS}); 982 {$\nu_{asym(C-S)}$}; 608 {$\nu_{sym(C-S)}$}; 456 {$\nu_{asym(S-Sn)}$}; 418 {$\nu_{sym(S-Sn)}$}. ^{1}H NMR (δ, $CDCl_3$): 7.89–7.30 (Sn–C_6H_5); 5.19–5.15 (OC*H*O); 3.96–3.82 (OCH_2 and NCH_2); 3.40 (NCH_3). ^{13}C NMR (δ, $CDCl_3$): 201.5 (CS_2); 150.8–1278.2 (Sn–C_6H_5); 101.0 (OCHO); 64.9 (OCH_2); 60.0 (NCH_2); 45.2 (NCH_3). ^{119}Sn NMR (δ, $CDCl_3$): −498.5 {$^1J(^{119}Sn-^{13}C)$ = 791 Hz, $^2J(^{119}Sn-^1H)$ = 82.3 Hz}. δ (mm s^{-1}): 1.41; Δ (mm s^{-1}): 2.78. Analysis for $C_{24}H_{40}N_2O_4S_4Sn$: found (calc.) 43.88 (43.85); 4.61 (4.60); 4.27 (4.26).

3.4. Biological tests

3.4.1. Filamentous fungi

A. flavus (CCT 4952) was obtained from Tropical Collection Culture, S.P. (Brazil). *A. niger* (NRRL 3), *A. parasiticus* (ATCC 15517), *P. citrinum* (ATCC 756) and *C. senegalensis* (LABB 31) were obtained from ARS Culture Collection (NRRL, USA), American Type Culture Collection (ATCC, USA) and Biotechnology and Bioassays Laboratory (LABB, MG, Brazil). They were kept in potato dextrose agar (PDA) under refrigeration at 7 °C. The tests were performed in Broth Heart Infusion (BHI) medium. The fungal spores were counted in a Neubauer chamber. Dilutions were carried to achieve the required final concentration of spores of 5.0×10^3 spores mL^{-1}.

3.4.2. Bacteria

Gram-positive bacterium *S. aureus* (ATCC 25923), *L. monocytogenes* (ATCC 15313), *B. cereus* (ATCC 11778), *S. sanguinis* (ATCC 49456), and Gram-negative bacterium *E. coli* (ATCC 25723), *C. freundii* (ATCC 8090), *S. typhimurium* (ATCC 13311), *P. aeruginosa* (ATCC 27853) were obtained from American Type Culture Collection (ATCC, USA). The bacterial strains, stored in broth heart infusion (BHI) medium, were sub-cultured for testing in the same medium and incubated at 37 °C for 24 h. The concentration of cells in the final bacterial inoculum was of 4.16 x10^3 cells mL^{-1}, determined by spectrophotometric method. The activity of the complexes was evaluated in final concentrations ranging from 250 to 0.12 mg mL^{-1} in microdilution plates with 96-wells according to Gupta and Zacchino [45]. The dithiocarbamate organotin(IV) complexes, nystatin and miconazole nitrate were prepared as 12.5 mg mL^{-1} stock solutions in DMSO. Subsequently, the stock solutions were diluted in BHI obtaining 500 μg mL^{-1} solutions. Further dilutions of each antifungal agent were performed in BHI medium. The wells of microdilution plates were filled with 100 μL of solutions with decreasing concentrations of the antimicrobial agent in culture medium. Then 100 μL of the solution containing the standardized inocula were added and the microplates were incubated at 37 °C for 24 and 48 h for anti-bacterial and 48 h for anti-fungal tests. Controls were performed for evaluating the growth of microorganisms in culture medium without any compound (positive control) and with the compounds to assure the sterility of the culture medium. Tests with the reference compounds, nystatin, miconazole nitrate, chloramfenicol and ampicillin, were also carried out (negative controls). The experiments were carried out in triplicate and the absorbances were determined on an ELISA tray reader (Thermoplate, Brazil) at fixed wavelength of 492 nm. MICs were calculated based on the quantity of the microorganism present after the experiments, i.e., the lowest concentration of compounds that resulted in a 50% (MIC_{50}) or 90% (MIC_{90}) reduction of growth compared with the control growth in the culture medium free of the test compound.

4. Conclusions

Complexes **(1)**–**(6)** were prepared and fully characterized by a series of spectroscopic methods. The best fungicide activity, in terms of IC_{90} and IC_{50}, were displayed by those complexes with R = Ph or Bu, [$SnPh_2\{S_2CNMe(R^1)_2\}_2$] **(3)**; [$Sn(n\text{-}Bu)_2\{S_2CNMe(R^2)_2\}_2$] **(5)** and [$SnPh_2\{S_2CNMe(R^2)_2\}_2$] **(6)**, {$R^1$ = $CH_2CH(OMe)_2$, and R^2 = 2-methyl-1,3-dioxolane}. It was observed a higher activity compared to miconazole in the presence of filamentous fungus such as *A. flavus*, *A. niger*, *A. parasiticus* and *P. citrinum*. Complexes **(1)**–**(6)** were less active towards *S. aureus* and *E. Coli* than the control drug. Theoretical calculations (SAR) served as support to the biocide assays, but revealed that

little differences in structure and properties might be responsible for the diverse behaviour of complexes **(1)**–**(6)** in biological media.

5. Supplementary data

Crystallographic data are available on request at Cambridge Crystallographic Data Centre on quoting the deposition numbers CCDC 883617, 883618, 883619, 883620, 883621 and 883622.

Acknowledgements

This work was supported by CNPq and FAPEMIG – Brazil.

References

[1] E.R.T. Tiekink, Tin dithiocarbamates: applications and structures, Appl. Organomet. Chem. 22 (2008) 533–550.
[2] I. Haiduc, in: T.J.M.J.A. McCleverty (Ed.), Comprehensive Coordination Chemistry II, Elsevier, Oxford, 2004, pp. 349–376.
[3] P.J. Heard, Main group dithiocarbamate complexes, in: Progress in Inorganic Chemistry, vol. 53, John Wiley & Sons Inc, New York, 2005, pp. 1–69.
[4] G. Hogarth, Transition metal dithiocarbamates: 1978–2003, in: Progress in Inorganic Chemistry, vol. 53, John Wiley & Sons Inc, New York, 2005, pp. 71–561.
[5] F.W. Sunderman, Efficacy of sodium diethyldithiocarbamate (dithiocarb) in acute nickel carbonyl poisoning, Ann. Clin. Lab. Sci. 9 (1979) 1–10.
[6] D.L. Bodenner, P.C. Dedon, P.C. Keng, R.F. Borch, Effect of diethyldithiocarbamate on cis-diamminedichloroplatinum(II)-induced cytotoxicity, DNA cross-linking, and gamma-glutamyl-transferase transpeptidase inhibition, Cancer Res. 46 (1986) 2745–2750.
[7] J.J. Suh, H.M. Pettinati, K.M. Kampman, C.P. O'Brien, The status of disulfiram – a half of a century later, J. Clin. Psychopharmacol. 26 (2006) 290–302.
[8] B. Cvek, Z. Dvorak, Targeting of nuclear factor-kappa B and proteasome by dithiocarbamate complexes with metals, Curr. Pharm. Des. 13 (2007) 3155–3167.
[9] P.J. Nieuwenhuizen, J. Reedijk, M. Van Duin, W.J. McGill, Thiuram- and dithiocarbamate-accelerated sulfur vulcanization from the chemist's perspective; methods, materials and mechanisms reviewed, Rubber Chem. Technol. 70 (1997) 368–429.
[10] M. Cicotti, Compound class: alkylenebis(dithiocarbamates), in: Handbook of Residue Analytical Methods for Agrochemical, vol. 2, Wiley, Chichester, 2003, pp. 1089–1098.
[11] D. Fan, M. Afzaal, M.A. Mallik, C.Q. Nguyen, P. O'Brien, P.J. Thomas, Using coordination chemistry to develop new routes to semiconductor and other materials, Coord. Chem. Rev. 251 (2007) 1878–1888.
[12] M.S. Vickers, J. Cookson, P.D. Beer, P.T. Bishop, B. Thiebaut, Dithiocarbamate ligand stabilised gold nanoparticles, J. Mater. Chem. 16 (2006) 209–215.
[13] Y.W. Koh, C.S. Lai, A.Y. Du, E.R.T. Tiekink, K.P. Loh, Growth of bismuth sulfide nanowire using bismuth tris-xanthate single source precursors, Chem. Mater. 15 (2003) 4544–4554.
[14] G. Barone, T. Chaplin, T.G. Hibbert, A.T. Kana, M.F. Mahon, K.C. Molloy, I.D. Worsley, I.P. Parkin, L.S. Price, Synthesis and thermal decomposition studies of homo- and heteroleptic tin(IV) thiolates and dithiocarbamates: molecular precursors for tin sulfides, J. Chem. Soc., Dalton Trans. (2002) 1085–1092.
[15] A.G. Davies, M. Gielen, K.H. Pannell, E.R.T. Tiekink, Tin Chemistry – Fundamentals, Frontiers and Applications, Wiley, Chichester, 2008.
[16] H. Tlahuext, R. Reyes-Martinez, G. Vargas-Pineda, M. Lopez-Cardoso, H. Hopfl, Molecular structures and supramolecular association of chlorodiorganotin(IV) complexes with bis- and tris-dithiocarbamate ligand, J. Organomet. Chem. 696 (2011) 693–701.
[17] N. Awang, I. Baba, B.M. Yamin, S.W. Ng, Di-n-butylbis(N-cyclohexyl-N-ethyldithiocarbamato-kappa 2 S, S′)tin(IV), Acta Crystallogr. Sect. E. Struct Rep. Online 66 (2010). M938–U753.
[18] A. Husain, S.A.A. Nami, K.S. Siddiqi, Synthesis, characterization and biocidal activities of heterobimetallic complexes having tin(IV) as a padlock, J. Mol. Struct. 970 (2010) 117–127.
[19] J.P. Fuentes-Martinez, I. Toledo-Martinez, P. Roman-Bravo, P.G.Y. Garcia, C. Godoy-Alcantar, M. Lopez-Cardoso, H. Morales-Rojas, Diorganotin(IV) dithiocarbamate complexes as chromogenic sensors of anion binding, Polyhedron 28 (2009) 3953–3966.
[20] A. Normah, K.N. Farahana, B. Ester, H. Asmah, N. Rajab, A.A. Halim, Cytotoxic and genotoxic effect of triphenyltin(IV) benzylisopropyldithiocarbamate in thymoma murine cell line (WEHI 7.2), Res. J. Chem. Environ. 15 (2011) 544–549.
[21] R. Singh, N.K. Kaushik, Spectral and thermal studies with anti-fungal aspects of some organotin(IV) complexes with nitrogen and sulphur donor ligands derived from 2-phenylethylamine, Spectrochim. Acta A Mol. Biomol. Spectrosc. 71 (2008) 669–675.
[22] E. Santacruz-Juarez, J. Cruz-Huerta, I.F. Hernandez-Ahuactzi, R. Reyes-Martinez, H. Tlahuext, H. Morales-Rojas, H. Hopfl, 24-and 26-Membered macrocyclic diorganotin(IV) bis-dithiocarbamate complexes with N, N′-disubstituted 1,3-and 1,4-bis(aminomethyl)benzene and 1,1′-bis(aminomethyl)ferrocene as spacer groups, Inorg. Chem. 47 (2008) 9804–9812.
[23] S. Shahzadi, S. Ali, M. Fettouhi, Synthesis, spectroscopy, in vitro biological activity and X-ray structure of (4-methylpiperidine-dithiocarbamato-S, S′) triphenyltin(IV), J. Chem. Crystallogr. 38 (2008) 273–278.
[24] D.C. Menezes, G.M. de Lima, F.A. Carvalho, M.G. Coelho, A.O. Porto, R. Augusti, J.D. Ardisson, Synthesis of phase-pure SnS particles employing dithiocarbamate organotin(IV) complexes as single source precursors in thermal decomposition experiments, Appl. Organomet. Chem. 24 (2008) 650–655.
[25] D.C. Menezes, G.M. de Lima, A.O. Porto, M.P. Ferreira, J.D. Ardisson, R.A. Silva, An interesting temperature dependence of the thermal decomposition of dithiocarbamate tin(IV) complexes molecular precursors for tin sulphides, Main Group Met. Chem. 30 (2007) 49–61.
[26] D.C. Menezes, G.M. de Lima, G.S. de Oliveira, A.V. Boas, A.M.A. Nascimento, F.T. Vieira, In vitro antibacterial activity of dithiocarbamate organotin(IV) complexes towards *Staphylococcus aureus*, Main Group Met. Chem. 31 (2008) 21–27.
[27] D.C. Menezes, F.T. Vieira, G.M. de Lima, A.O. Porto, M.E. Cortes, J.D. Ardisson, T.E. Albrecht-Schmitt, Tin(IV) complexes of pyrrolidinedithiocarbamate: synthesis, characterisation and antifungal activity, Eur. J. Med. Chem. 40 (2005) 1277–1282.
[28] J.S. White, J.M. Tobin, J.J. Cooney, Organotin compounds and their interactions with microorganisms, Can. J. Microbiol. 45 (1999) 541–554.
[29] J.J. Cooney, S. Wuertz, Toxic effects of tin-compounds on microorganisms, J. Ind. Microbiol. 4 (1989) 375–402.
[30] D.C. Menezes, F.T. Vieira, G.M. de Lima, J.L. Wardell, M.E. Cortes, M.P. Ferreira, M.A. Soares, A.V. Boas, The in vitro antifungal activity of some dithiocarbamate organotin(IV) compounds on *Candida albicans* – a model for biological interaction of organotin complexes, Appl. Organomet. Chem. 22 (2008) 221–226.
[31] R.C. Poller, The Chemistry of Organotin Compounds, Logos Press Limited, London, 1970.
[32] F. Bonati, R. Ugo, Organotin(4) N, N-disubstituted dithiocarbamates, J. Organomet. Chem. 10 (1967) 257–268.
[33] L. Ronconi, L. Giovagnini, C. Marzano, F. Bettio, R. Graziani, G. Pilloni, D. Fregona, Gold dithiocarbamate derivatives as potential antineoplastic agents: design, spectroscopic properties, and in vitro antitumor activity, Inorg. Chem. 44 (2005) 1867–1881.
[34] H.L.M. Vangaal, J.W. Diesveld, F.W. Pijpers, J.G.M. Vanderlinden, ^{13}C NMR-spectra of dithiocarbamates. Chemical-shifts, carbon–nitrogen stretching vibration frequencies, and π-bonding in the NCS_2 fragment, Inorg. Chem. 18 (1979) 3251–3260.
[35] J. Holecek, M. Nadvornik, K. Handlir, A. Lycka, ^{13}C and ^{119}Sn NMR-spectra of di-normal-butyltin(IV) compounds, J. Organomet. Chem. 315 (1986) 299–308.
[36] T.P. Lockhart, W.F. Manders, J.J. Zuckerman, Structural investigations by solid-state ^{13}C NMR. Dependence of $|^1J(^{119}Sn, ^{13}C)|$ on the Me–Sn–Me angle in methyltin(IV), J. Am. Chem. Soc. 107 (1985) 4546–4547.
[37] T.P. Lockhart, W.F. Manders, Structure determination by NMR spectroscopy. Correlation of $|^2J(^{119}Sn, ^1H)|$ and the Me–Sn–Me angle in methyltin(IV) compounds, Inorg. Chem. 25 (1986) 892–895.
[38] T.P. Lockhart, W.F. Manders, Solid-state ^{13}C NMR investigation of methyltin(IV) compounds. Correlation of NMR parameters with molecular-structure, J. Am. Chem. Soc. 109 (1987) 7015–7020.
[39] H.A. Bent, An appraisal of valence-bond structures and hybridization in compounds of the 1st-row elements, Chem. Rev. 61 (1961) 275–311.
[40] S. Basu, A. Mizar, T. Baul, E. Rivarola, ^{119}Sn Mössbauer characterization of self assembled organotin(IV) complexes with Schiff bases containing amino acetate skeletons, Hyperfine Interact. 185 (2008) 95–102.
[41] M. Gielen, H. Dalil, M. Biesemans, B. Mahieu, D. de Vos, R. Willem, Di- and triorganotin derivatives of 3S,4S-3-[(R)-1-(tert-butyl-dimethylsilyloxy)ethyl]-4-[(R)-carboxyethyl]-2-azetidinone: synthesis, characterization and in vitro antitumour activity, Appl. Organomet. Chem. 13 (1999) 515–520.
[42] A. Bondi, Van der Waals volumes and radii, J. Phys. Chem. 68 (1964) 441–451.
[43] N. Singh, S. Bhattacharya, Synthesis and characterization of some triorgano, diorgano, monoorganotin and a triorgano lead heteroaromatic dithiocarbamate complexes, J. Organomet. Chem. 700 (2012) 69–77.
[44] (a) F. Shaheen, Zia-ur -Rehman, S. Ali, A. Meetsma, Structural properties and antibacterial potency of new supramolecular organotin(IV) dithiocarboxylates, Polyhedron 31 (2012) 697–703;
(b) N.F. Kamaluduin, I. Baba, N. Awang, M.I.M Tahir, E.R.T.Tiekink, Acta Crystallogr. Sect. E. Struct Rep. Online, 68 M79–M80.
[45] A.S. Zacchino, M.P. Gupta, Manual de técnicas in vitro para la detección de compuestos antifúngicos, Corpus Editorial y Distribuidora, Rosario, 2007, 85–99.
[46] H.K. Munayyer, P.A. Mann, A.S. Chau, T. Yarosh-Tomaine, J.R. Greene, R.S. Hare, L. Heimark, R.E. Palermo, D. Loebenberg, P.M. McNicholas, Posaconazole is a potent inhibitor of sterol 14 alpha-demethylation in yeasts and molds, Antimicrob. Agents Chemother. 48 (2004) 3690–3696.
[47] K.M. Brumfield, J.V. Moroney, T.S. Moore, T.A. Simms, D. Donze, Functional characterization of the *Chlamydomonas reinhardtii* ERG3 ortholog, a gene involved in the biosynthesis of ergosterol, PLoS One 5 (2010) e8659, 1–10.
[48] D.J. Sheehan, C.A. Hitchcock, C.M. Sibley, Current and emerging azole antifungal agents, Clin. Microbiol. Rev. 12 (1999) 40–79.
[49] F.T. Vieira, D.C. Menezes, G.M. de Lima, J.L. Wardell, M.E. Cortes, G.A.B. Silva, A. Vilas-Boas, J. Maia, Effect of diorganotin(IV) carboxylate complexes, [N-(2-carboxyphenyl) salicylideneiminato]dimethyltin(IV), bis(μ_3-oxo)bis(μ-O-

aminobenzoato-O, O′)bis(O-aminobenzoato)tetrakis[dimethyltin(IV)] and bis(O-aminobenzoato-O, O′)di-n-butyltin(IV), on the membrane of *Candida albicans* cells – a mechanistic investigation of the antifungal activity of organotin complexes, Appl. Organomet. Chem. 22 (2008) 433–439.
[50] S.T.M. Orr, S.L. Ripp, T.E. Ballard, J.L. Henderson, D.O. Scott, R.S. Obach, H. Sun, A.S. Kalgutkar, Mechanism-based inactivation (MBI) of cytochrome P450 enzymes: structure–activity relationships and discovery strategies to mitigate drug–drug interaction risks, J. Med. Chem. 55 (2012) 4896–4933.
[51] G.L. Parrilha, J.G. da Silva, L.F. Gouveia, A.K. Gasparoto, R.P. Dias, W.R. Rocha, D.A. Santos, N.L. Speziali, H. Beraldo, Pyridine-derived thiosemicarbazones and their tin(IV) complexes with antifungal activity against *Candida* spp, Eur. J. Med. Chem. 46 (2011) 1473–1482.
[52] M.A. Soares, J.A. Lessa, I.C. Mendes, J.G. Da Silva, R.G. dos Santos, L.B. Salum, H. Daghestani, A.D. Andricopulo, B.W. Day, A. Vogt, J.L. Pesquero, W.R. Rocha, H. Beraldo, N-4-phenyl-substituted 2-acetylpyridine thiosemicarbazones: cytotoxicity against human tumor cells, structure–activity relationship studies and investigation on the mechanism of action, Bioorg. Med. Chem. 20 (2012) 3396–3409.
[53] C. Hansch, B. Bonavida, A.R. Jazirehi, J.J. Cohen, C. Milliron, A. Kurup, Quantitative structure–activity relationships of phenolic compounds causing apoptosis, Bioorg. Med. Chem. 11 (2003) 617–620.
[54] CrysAlis PRO, Oxford Diffraction Ltd., Version 1.171.34.34 (release 07-07-2010 CrysAlis171.NET) (compiled Jul 7 2010, 16:04:54).
[55] G.M. Sheldrick, SHELXS-97. Program for the Solution of Crystal Structures, University of Göttingen, Germany, 1997.
[56] G.M. Sheldrick, SHELXL-97. Program for Crystal Structure Refinement, University of Göttingen, Germany, 1997.
[57] L.J. Farrugia, ORTEP-3 for Windows – a version of ORTEP-III with a graphical user interface (GUI), J. Appl. Cryst. 30 (1997) 565–566.
[58] R.G. Parr, W. Yang, Density-functional Theory of Atoms and Molecule, Oxford University Press, Oxford, 1989.
[59] A.D. Becke, Density-functional thermochemistry. III. The role of exact exchange, J. Chem. Phys. 98 (1993) 5648–5652.
[60] C.T. Lee, W.T. Yang, R.G. Parr, Development of the Colle-Salvetti correlation-energy formula into a functional of the electron density, Phys. Rev. B 37 (1988) 785–789.
[61] R. Ditchfie, W.J. Hehre, J.A. Pople, Self-consistent molecular-orbital methods. IX. An extended Gaussian-type basis for molecular-orbital studies of organic molecules, J. Chem. Phys. 54 (1971) 724–728.
[62] W.J. Hehre, R. Ditchfie, J.A. Pople, Self-consistent molecular-orbital methods. XII. Further extensions of Gaussian-type basis sets for use in molecular-orbital studies of organic-molecules, J. Chem. Phys. 56 (1972) 2257–2261.
[63] P.J. Hay, W.R. Wadt, Ab initio effective core potentials for molecular calculations. Potentials for K to Au including the outermost core orbitals, J. Chem. Phys. 82 (1985) 299–310.
[64] M.J. Frisch, G.W. Trucks, H.B. Schlegel, G.E. Scuseria, M.A. Robb, J.R. Cheeseman, J.A.M Jr., T. Vreven, K.N. Kudin, J.C. Burant, J.M. Millam, S.S. Iyengar, J. Tomasi, V. Barone, B. Mennucci, M. Cossi, G. Scalmani, N. Rega, G.A. Petersson, H. Nakatsuji, M. Hada, M. Ehara, K. Toyota, R. Fukuda, J. Hasegawa, M. Ishida, T. Nakajima, Y. Honda, O. Kitao, H. Nakai, M. Klene, X. Li, J.E. Knox, H.P. Hratchian, J.B. Cross, V. Bakken, C. Adamo, J. Jaramillo, R. Gomperts, R.E. Stratmann, O. Yazyev, A.J. Austin, R. Cammi, C. Pomelli, J.W. Ochterski, P.Y. Ayala, K. Morokuma, G.A. Voth, P. Salvador, J.J. Dannenberg, V.G. Zakrzewski, S. Dapprich, A.D. Daniels, M.C. Strain, O. Farkas, D.K. Malick, A.D. Rabuck, K. Raghavachari, J.B. Foresman, J.V. Ortiz, Q. Cui, A.G. Baboul, S. Clifford, J. Cioslowski, B.B. Stefanov, G. Liu, A. Liashenko, P. Piskorz, I. Komaromi, R.L. Martin, D.J. Fox, T. Keith, M.A. Al-Laham, C.Y. Peng, A. Nanayakkara, M. Challacombe, P.M.W. Gill, B. Johnson, W. Chen, M.W. Wong, C. Gonzalez, J.A. Pople, Gaussian 03, Revision C.02, Gaussian, Inc, Wallingford CT, 2004.
[65] Calculator Plugins Were Used for Structure Property Prediction and Calculation, MarvinView 5.10.3, ChemAxon, 2012.http://www.chemaxon.com.